

EFFECTIVE TENSILE STRESS-STRAIN
CHARACTERISTICS FOR REINFORCED CONCRETE

L. Hwang, Graduate Student, Department of Civil Engineering,
University of Manitoba, Winnipeg, Manitoba.

S. Rizkalla, Associate Professor, Department of Civil Engineering,
University of Manitoba, Winnipeg, Manitoba.

ABSTRACT

After cracking of reinforced concrete structures, the concrete continues to contribute to the effective stiffness of structures, due to tension stiffening. This paper proposes an elastic-plastic-softening constitutive relationship for reinforced concrete developed for analysis of reinforced and/or prestressed concrete structures. The model is based on a large experimental program conducted at the University of Manitoba to determine the behavior of concrete segments reinforced in two directions and loaded in pure membrane tension. The segments were designed to include different parameters which could affect the cracking behavior, such as concrete cover, concrete thickness, percentage of steel, and spacing between transverse reinforcement. From the results of these tests, an expression for the cracking strength was determined and related to standard split and compressive cylinder strengths.

The proposed constitutive relationship includes the behavior of concrete in the pre- and post-cracking regions. The model assumes a linear relationship up to the cracking strength and an exponential relationship after cracking of the concrete. The proposed model was applied and the results were compared to a measured value from the experimental program and also with independent experimental results for uniaxially and biaxially loaded prestressed concrete segments in tension. It has been demonstrated that the proposed constitutive relationship permits an excellent prediction of the deformation of reinforced and prestressed concrete members subjected to tensile membrane loading.

1. INTRODUCTION

A valid constitutive model to describe concrete behavior under tension and compression is a fundamental requirement for nonlinear analysis of reinforced concrete structures. To date, the behavior of concrete under compression has been well defined. However, very little information is available to describe the response of concrete in tension, and in particular, the post-cracking response in the presence of steel reinforcement.

Cracking of concrete due to applied tensile stresses is considered to be one of the most important parameters influencing the nonlinear re-

sponse of reinforced concrete structures. For plain concrete, formation of cracks is a brittle process and the strength in the tension loading abruptly goes to zero. In the presence of reinforcements, which bridge the concrete cracks, the tension mechanism becomes quite different. After cracking of reinforced concrete structures, the concrete continues to contribute to the effective stiffness of structures, due to the tension stiffening effect of concrete between cracks.

The tension "cut-off" model for concrete has been used by many investigators (2,4,6,16,18) in the nonlinear analysis of reinforced concrete structures. However, Gilbert and Warner (8) indicate that using such a model will significantly affect the stiffness and could result in a 100 per cent overestimation of a reinforced concrete slab's deflection. A similar comparison conducted by Kulicki and Kostem (12) indicated that the tension "cut-off" model fails to describe the response satisfactorily and tends to overestimate the strains and, consequently, displacements (7).

Recently, the effect of these cracks have been accommodated in a general constitutive model for reinforced concrete. This model assumes that the concrete remains continuous in the post-cracking region (11,13). This accommodation was accomplished by "smearing out" the cracks in a continuous fashion which is more convenient for obtaining load-deformation behavior using any numerical technique.

The objective of this paper is to propose a full description of an elastic-plastic-softening constitutive relationship for reinforced concrete developed for analysis of reinforced and/or prestressed concrete structures. The model will include the magnitude of the maximum tensile stress, and corresponding tensile strain, which will initiate crack development. The concrete cracking strength is related to the standard ultimate compressive strength and split strength.

The proposed model is based on a large experimental program involving reinforced concrete segments tested in tension. The specimens were designed to include different parameters which could affect the cracking behavior, such as concrete cover, concrete thickness, percentage of steel, and spacing between transverse reinforcements. The proposed constitutive relationship was applied and the results were compared to measured values from the experimental program, and also with independent experimental results for uniaxially and biaxially loaded prestressed concrete segments in tension (11).

2. TEST SPECIMENS

All segments were reinforced in two directions with deformed bars. Longitudinal reinforcements were spaced at 3" (76 mm) centre to centre and extended 11" (280 mm) beyond each end of the specimen, as shown in Figure 1. The main variables in the test series were concrete cover, c , percentage of steel in the direction of the applied load, p , concrete thickness of the specimen, t , and spacing between transverse reinforcement, S_R , as given in Table 1.

All concrete used in fabrication of the segments was designed for a nominal ultimate strength of 5,000 psi (34.5 MPa) and was mixed in the laboratory. Control cylinders 6" x 12" (152 x 305 mm) were cast at the same time with the specimens in order to relate the specimen behavior to standard material test results. Material tests were carried out at the time of testing of the main specimen and consisted of compression tests to measure the ultimate compressive strength, f'_c , and modulus of elasticity, E_c , and split cylinder tests to measure split strength, f'_{sp} . For each specimen, samples of the steel bars were tested for tension to determine yield strength, f_y , ultimate strength, f_u , and modulus of elasticity, E_s . The values of f'_{sp} , f'_c , E_c and f_y are summarized in Table 2.

The load was applied using a 600,000 lb. (2670 KN) capacity universal testing machine. Load was transmitted from the loading machine to the specimen by using specially designed end fittings, as shown in Figure 2. The end fittings were very rigid, in order to achieve uniformity of loads from the machine to each load cell. Each reinforcing bar was connected to a separate, specially designed load cell, which was used to adjust the load.

During testing, a continuous record of deformation over a 30" (762 mm) gauge length was made using a linear variable differential transducer (LVDT) as shown in Figure 2. As well, readings for mechanical strain gauges were recorded. Crack patterns were marked as they formed and propagated. Crack locations and crack width measurements were recorded. Testing was terminated when the load approached the yield point. A detailed description of the instrumentation, testing procedure, and test results is contained in Reference (9).

3. CONCRETE SPLIT STRENGTH

Recently, Carino and Lew (3) concluded that the ACI (1) expression:

$$f'_{sp} = 6.7 \sqrt{f'_c} \quad (\text{psi}) \quad \dots \quad \text{Equation (1)}$$

for predicting the concrete split strength tends to overestimate the strength for low compressive strength concrete and to underestimate the strength for high compressive strength concrete. Based on regression analysis of 798 test data, Mirza, et al. (14), also concluded that the ACI equation gives conservative estimates of the splitting strength of concrete and proposed the following expression:

$$f'_{sp} = 4.4 f'_c{}^{0.55} \quad (\text{psi}) \quad \dots \quad \text{Equation (2)}$$

A new expression proposed by Carino and Lew (3), to estimate the concrete split strength in terms of the ultimate compressive strength is as follows:

$$f'_{sp} = 1.15 (f'_c)^{0.71} \quad (\text{psi}) \quad \dots \quad \text{Equation (3)}$$

To eliminate the constant value in Equation (3), they introduced the following simplified form:

$$f'_{sp} = (f'_c)^{0.73} \cdot (\text{psi}) \dots\dots\dots \text{Equation (4)}$$

The relationship based on Equations (1),(2),(3) and (4) were compared to the measured values from the experimental program reported herein, and to values obtained from Reference (7) are shown in Figure 3. The comparisons suggest an underestimation of the split strength by ACI (Eq. (1)), and Mirza,et al.(Eq. (2)), beyond a concrete compressive strength of 6,000 psi (41.4 MPa). Both equations given by Carino and Lew (Eqs.(3) and (4)) show high accuracy in predicting the split strength of concrete and cover much wider ranges of f'_c .

4. CONCRETE CRACKING STRENGTH

The cracking strength of concrete is affected by many factors, such as loading rate, moisture content, curing conditions, size effect, and percentage of steel. The strength is also affected by the mode of crack development, and will be different, depending on whether flexural or direct tensile cracking has taken place. The different factors which might affect the cracking behavior of reinforced concrete structures, such as concrete cover, bar spacing, transverse reinforcements, and reinforcement ratio, may all be expected also to have an influence on the cracking strength of concrete.

Based on experimental results, Chitnuyanondh (1) introduced two expressions for predicting the concrete cracking strength, f_{cr} , in terms of the split strength, f'_{sp} and ultimate compressive strength, f'_c , as follows:

$$f_{cr} = 0.6 f'_{sp} \cdot (\text{psi}) \dots\dots\dots \text{Equation (5)}$$

and

$$f_{cr} = 3.65 \sqrt{f'_c} \cdot (\text{psi}) \dots\dots\dots \text{Equation (6)}$$

Chitnuyanondh inferred that the low magnitude of cracking strength, as compared to the split strength, is mainly due to the rate of loading and volume effect.

The cracking load, P_{cr} , for all the tested specimens was determined from load-strain plots to be the "intersection point" of the tangent lines to the pre-cracking and post-cracking response as shown in Figure 4, for a typical load-strain relationship, using specimen No. 2 as an example. This was usually a well-defined point, since both pre-cracking and post-cracking responses were essentially linear.

The measured strains were determined as the average strains obtained from three 8" (200 mm) Demec gauge lengths in the direction of the applied load within a 24" (610 mm) length on the face of the specimen, as shown in Figure 2. The cracking strength, f_{cr} , was determined by computing the stress on the specimen surface as:

$$f_{cr} = \frac{P_{cr}}{A_t} \cdot \dots\dots\dots \text{Equation (7)}$$

where A_t is the appropriate transformed area of the specimen cross-section, f_{cr} is considered to be the "true" cracking strength of the concrete as exhibited in the reinforced concrete segment. The values of the cracking load, P_{cr} , and the corresponding tensile strength, f_{cr} , and cracking strain, ϵ_{cr} , for all the specimens are listed in Table 2. Various ratios of these values are shown in Table 3 together with mean values and standard deviations. The "true" cracking strength, f_{cr} , for all the specimens were compared to the concrete split strengths in Figure 5, which shows an average value of 0.6. This indicates that the "true" cracking strength in the tested specimen had a mean value of only 60 per cent of that which would be predicted from a split cylinder test.

If the ratio of 0.6 is combined with Carino and Lew's expressions, an expression of the "true" cracking strength can be obtained as follows:

$$f_{cr} = 0.6(f'_c)^{0.73} \text{ (psi) ,} \quad \dots\dots\dots \text{Equation (8)}$$

and

$$f_{cr} = (f'_c)^{2/3} \text{ (psi) .} \quad \dots\dots\dots \text{Equation (9)}$$

The calculated cracking strength was also compared to the ultimate compressive strength in Figure 6. The mean value of 4.4, which was obtained, suggests that

$$f_{cr} = 4.4\sqrt{f'_c} \text{ (psi) .} \quad \dots\dots\dots \text{Equation (10)}$$

The "true" tensile strengths based on Equations (8), (9), and (10) were compared to the measured values in Figure 7, and gave a satisfactory agreement.

5. EFFECTIVE TENSILE STRESS-STRAIN CURVE OF REINFORCED CONCRETE

A load-average gross strain for a typical specimen is shown in Figure 4, where Specimen 2 was used as an example. In the same figure, the response based on the steel alone is shown as a straight line. The shaded area represents the concrete contribution in the pre- and the post-cracking ranges.

At any given load, P , and corresponding average gross strain, ϵ_m , the force carried by the concrete, P_c , can be determined from the test results as

$$P_c = P - A_s E_s \epsilon_m \text{ ,} \quad \dots\dots\dots \text{Equation (11)}$$

where A_s and E_s are the area and modulus of elasticity of the steel, respectively. Thus the effective tensile stress, f_t , for this given average strain, ϵ_m , can be determined as follows:

$$f_t = \frac{P_c}{A_c} \text{ ,} \quad \dots\dots\dots \text{Equation (12)}$$

where A_c is the area of concrete. Using Equations (11) and (12), the effective tensile stress was calculated for all the specimens with transverse reinforcements located at 3" (76 mm) centre-to-centre and variable concrete

cover, reinforcement ratio, and concrete thickness, and is shown in Figure 8. In spite of the considerable scatter, the general trend of linear relation prior to cracking and a gradual post-cracking softening in the effective stress-strain curve is clearly evident.

Based on Figure 8, the proposed stress-strain curve assumes a linear relationship up to the concrete cracking strength, f_{cr} . Thus, for a given value of the modulus of elasticity of concrete, E_c , the cracking strain, ϵ_{cr} , can be determined based on the proposed linear response before the initiation of the first crack. The magnitude of the modulus of elasticity in tension can be assumed to equal the initial modulus of elasticity of concrete in compression, since the difference between the two moduli is insignificant, as was proposed by Johnson (10).

After cracking, where the average gross strain, ϵ_m , exceeds the cracking strain, ϵ_{cr} , the proposed stress-strain curve can be represented by the following exponential function up to average strain equal to the yield strain of steel.

$$f_t = f_{cr} e^{-(\epsilon_m - \epsilon_{cr}) \times 10^3}, \quad \dots \dots \dots \text{Equation (13)}$$

where f_t is the effective tensile stress of the concrete at any given average gross strain in tension, ϵ_m , and f_{cr} is the cracking strength of concrete at which the first crack is initiated. The effectiveness of this relationship in simulating the behavior of various segments can be determined by using this curve as input for any numerical analysis solution and comparing the output with measured values.

In Figures 9(a) and 9(b) the constitutive models proposed by Chitnuy-anondh (7) and Vecchio (17) are compared to the experimental results. The comparisons suggest very clearly that both models overestimate the response of reinforced concrete. This observation agrees with Chen's conclusion (5) that the aggregate interlocking effect in shear tends to overestimate the concrete stress, compared to that obtained from uniaxial tension tests. Koziak and Murray (11) also indicated that the effective tensile stress-strain response based on prestressed concrete segments is significantly higher than that obtained from reinforced concrete specimens.

To study the effect of concrete cover, concrete thickness, and steel reinforcement ratio, the measured effective stress-strains of specimens with variable quantities of the above functions were compared to values obtained using the proposed constitutive model in Figures 9(a) and 9(b). The comparison clearly indicated that the above mentioned variables have an insignificant effect on the proposed model.

The effect of the spacing between the transverse reinforcement steel bars, S_R , was investigated as shown in Figure 10(a), which shows a considerable scatter. However, the behavior can be explained by using the dimensionless parameter, R , introduced in Reference (15), where,

$$R = \frac{S_R}{S_m}, \quad \dots \dots \dots \text{Equation (14)}$$

where S_m is the predicted average crack spacing without the presence of transverse reinforcement, and S_R is the spacing between transverse reinforcements.

Values of R significantly lower or greater than one, as given in Table 3 for specimens 2, 2A, 2B, and 2C indicate that the transverse reinforcement has insignificant effect on the crack pattern, thus the proposed model is capable of predicting the response accurately, as shown in Figure 10(a).

Values of R slightly lower or greater than one, indicate that the transverse reinforcement does influence the crack spacing. For specimens 4A, 4B, and 4C, the value of R is 0.94 and the cracks were located at each transverse reinforcement bar, i.e., at a distance less than the expected value. Consequently, the concrete would contribute less in comparison to the proposed model as shown in Figure 10(a), for these specimens. For specimens 6A, 6B, and 6C, all having an R value of 1.42, the cracks were located at a distance greater than the predicted values and less cracks were found. This will consequently cause the concrete to contribute more in tension to the proposed model, which consistently underestimates the response for these specimens, as shown in Figure 10(a).

Similar behaviors are also observed for specimens with concrete covers equal to 1.50" (38 mm), as shown in Figure 10(b). The proposed stress-strain curve underestimates the response in these specimens. Should the cracking strength, f_{cr} , be more accurately assessed, better prediction can be achieved.

6. SIMULATION OF EXPERIMENTAL BEHAVIOR

If the proposed constitutive model in tension shown in Figure 8 is to have validity, an analytical model of a segment test should produce results which agree with experimental observations when the aforementioned stress-strain properties are input to the analysis. If such a correlation can be obtained, it serves to verify the effectiveness of the material properties for use with the particular analytical method.

The material properties derived herein have been used in conjunction with a computer program developed in Reference (11). The response of the segment to a given set of strains is found by layering the segment through the thickness as shown in Figure 11, giving each layer appropriate properties and then integrating the responses from the individual layers to find the segment response. The constitutive relation of the reinforcing steel consists of the conventional two-part elastic-perfectly plastic curve. The value of f_{cr} was determined based on Equations (5) and (9).

Comparison between the computer analyses and experimental observations for segments 6 and 2B are shown in Figures 12 and 13. These specimens were reinforced in two directions and subjected to uniaxial membrane tensile forces. The two specimens have different concrete covers and material properties, and the transverse reinforcements were located 10.5" (267 mm) and 2" (50 mm) centre-to-centre, respectively.

Comparison between predicted results and measured values for two prestressed specimens tested in Reference (11), are shown in Figures 14 and 15. The first specimen was prestressed in one direction and loaded by uniaxial membrane tensile forces, while the second specimen was prestressed in two directions and subjected to biaxial membrane tensile forces. Again, the comparison is excellent and confirm the conclusion made by Kupfer, et al. (19), and Murray (7), that the biaxial tensile values are independent of the stress ratio and equal to the uniaxial tensile strength. The results also confirm that the proposed model is applicable for reinforced concrete, as well as prestressed concrete members loaded by membrane tension.

7. SUMMARY AND CONCLUSIONS

An experimental program to determine the behavior of reinforced concrete segments loaded in pure membrane tension has been described. Analysis of the results indicates that cracking of these segments is initiated at an average value of 60 percent of the split strength of concrete. Expressions for the split strength and for cracking strength of concrete are recommended. A detailed description of a constitutive model for concrete in tension, including pre- and post-cracking regions, has been proposed. It has been demonstrated that the proposed constitutive model permits an excellent prediction of the deformation of reinforced concrete and prestressed concrete subjected to tensile membrane forces.

8. ACKNOWLEDGEMENTS

This study was carried out in the Department of Civil Engineering at the University of Manitoba with financial assistance from the Natural Sciences and Engineering Research Council of Canada, and the University of Manitoba Research Board.

REFERENCES

1. ACI 318-77, 1977. Building Code Requirements for Reinforced Concrete, ACI Committee 318, American Concrete Institute, Detroit.
2. Buyukgzuk, O., 1977. Nonlinear Analysis of Reinforced Concrete Structures. Computer and Structures, Vol. 7, pp. 149-156.
3. Carino, N.J., and Lew, H.S., 1982. Re-examination of the Relation Between Splitting Tensile and Compressive Strength of Normal Weight Concrete. Journal of the American Concrete Institute, Vol. 79, No. 3, pp. 214-219.
4. Cedolin, L., Crutzen, Y.R.J., and Deli Poli, S., 1977. Triaxial Stress-Strain Relationship for Concrete. Journal of the Engineering Mechanics Division, ASCE, Vol. 103, No. EM3, Proc. Paper 12969, pp. 423-439.

5. Chen, W.F., and Saleeb, A.F., 1982. Constitutive Equations for Engineering Materials, Vol. 1, John Wiley and Sons.
6. Chen, W.F., Suzuki, Hiroyuki, and Chang, T.Y., 1980. End Effects of Pressure-Resistant Concrete Shells. Journal of the Structural Division, ASCE, Vol. 106, No. ST4, Proc. Paper 15316, pp.751-771.
7. Chitnuyanondh, L., Rizkalla, S., Murray, D.W., and MacGregor, J.G., 1979. An Effective Uniaxial Stress-Strain Relationship for Prestressed Concrete. Structural Engineering Report No. 74, Department of Civil Engineering, University of Alberta, Edmonton, Alberta.
8. Gibert, I.R., and Warner, R.F., 1978. Tension Stiffening in Reinforced Concrete Slabs. Journal of the Structural Division, ASCE, Vol. 104, No. ST12, Proc. Paper 14211, pp. 1885-1900.
9. Hwang, L.S., 1983. Behavior of Reinforced Concrete in Tension at Post-cracking Range. M.Sc. Thesis, Department of Civil Engineering, University of Manitoba, Winnipeg.
10. Johnson, J.W., 1929. Relationship Between Strength and Elasticity of Concrete in Tension and Compression. Bulletin 90, Engineering Experimental Station, Iowa State College, Ames, Iowa.
11. Koziak, B.D.P., and Murray, D.W., 1979. Analysis of Prestressed Concrete Wall Segments. Structural Engineering Report No. 78, Department of Civil Engineering, University of Alberta, Edmonton, Alberta.
12. Kukicki, J.H., and Kostem, C.N., 1972. The Inelastic Analysis of Reinforced and Prestressed Concrete Beams. Rep. No. 378 B.1, Fritz, Eng. Lab., Lehigh University, Bethlehem, PA.
13. Lin, C.S., and Scordelis, A.C., 1975. Nonlinear Analysis of R/C Shells of General Form. Journal of the Structural Division, ASCE, Vol. 101, No. ST3, Proc. Paper 11164, pp. 523-538.
14. Mirza, S.A., Hatzinikolas, M., and MacGregor, J.G., 1979. Statistical Descriptions of Strength of Concrete. Journal of the Structural Division. ASCE, Vol. 105, ST. 6., Proc. Paper 14628, pp.1021-1037.
15. Rizkalla, S.H., Hwang, L.S., and El Shahawi, M., 1983. Transverse Reinforcement Effects on Cracking Behavior of R.C. Members. Canadian Journal of Civil Engineering. (to be published).
16. Romstad, K.M., Taylor, M.A., and Herman, L.R., 1974. Numerical Biaxial Characterization for Concrete. Journal of the Engineering Mechanics Division. ASCE, Vol. 100, No. EMS, pp. 935-948.
17. Vecchio, F., and Collins, M.D., 1982. The Response of Reinforced Concrete to In-Plane Shear and Normal Stresses. Technical Report, University of Toronto, Department of Civil Engineering, Publication No. 82-03.

18. Wegmuller, A.W., 1977. Overload Behavior of Composite Steel Concrete Bridges, Journal of the Structural Division, Vol. 103, No. ST9, Proc. Paper 13227, pp. 1799-1819.
19. Kupfer, H.B., Hilsdorf, H.K., and Rush, M., 1969. Behavior of Concrete Under Biaxial Stresses. ACI Journal, No. 8, Vol. 66.

NOTATION

A_C	area of concrete in cross-section
A_S	cross-sectional area of reinforcing bars
A_t	transformed area of specimen cross-section
c	minimum cover to surface of bar (measured perpendicular to surface)
E_C	modulus of elasticity of concrete
E_S	modulus of elasticity of steel
f'_C	compressive strength of concrete
f_{cr}	cracking strength of concrete
f'_{sp}	tensile split strength of concrete
f_t	effective tensile stress in concrete
f_u	ultimate strength of steel
f_y	yield strength of steel
p	reinforcement ratio
P	axial load
P_C	load carried by concrete
P_{cr}	cracking load
R	S_R/S_m
S_m	predicted average crack spacing
S_R	spacing between transverse bars
t	concrete thickness
ϵ_{cr}	cracking strain in concrete
ϵ_m	average strain measured over a gauge length which includes several cracks
ϵ_{s2}	steel strain at a crack
ϵ_y	yield strain of steel

TABLE 1 VARIABLES CONSIDERED IN THE EXPERIMENTAL PROGRAM

Concrete Cover (in)	Steel Ratio	Concrete Thickness (in)	Specimen Number	X-Section Area (sq. in)	Reinf. Bar Size	Transverse Bar Spacing, S_R (in)
0.50	0.0147	5.0	T1A	60.0	#3	3.0
		7.0	T4A	84.0	10M	3.0
		10.0	T7A	110.0	#4	3.0
	0.0207	5.0	T2A	60.0	10M	3.0
		7.0	T5A	77.0	#4	3.0
		10.0	T8A	120.0	15M	3.0
	0.0294	5.0	T3A	55.0	#4	3.0
		7.0	T6A	84.0	15M	3.0
		10.0	T9A	120.0	#6	3.0
0.75	0.0147	5.0	T1B	60.0	#3	3.0
		7.0	T4B	84.0	10M	3.0
		10.0	T7B	110.0	#4	3.0
	0.0207	5.0	T2B	60.0	10M	3.0
		7.0	T5B	77.0	#4	3.0
		10.0	T8B	120.0	15M	3.0
	0.0294	5.0	T3B	55.0	#4	3.0
		7.0	T6B	84.0	15M	3.0
		10.0	T9B	120.0	#6	3.0
0.75	0.0147	7.0	2A,2B,2C	84.0	10M	2.0
			4A,4B,4C			4.0
			6A,6B,6C			6.0
			#1			8.5
			#2			
1.50	0.0147	7.0	#3	84.0	10M	2.0
			#4			4.0
			#5			6.0
			#6			10.5
			#7			

TABLE 2 MEASURED AND COMPUTED STRENGTHS AND CRACKING STRAIN OF CONCRETE SEGMENTS

Specimen Number	f'_{sp} (psi)	f'_c (psi)	E_c (ksi)	f_y (psi)	P_{cr} (kips)	f_{cr} (psi)	ϵ_{cr}^* x 10^{-6}
T1A	610	7600	4650	61800	24.5	380	60.3
T1B	610	7480	4530	63150	25.0	387	165.5
T2A	610	8510	4720	52500	27.6	417	53.8
T2B	630	7360	4800	52950	26.0	393	108.9
T3A	560	7330	4970	54300	25.0	399	77.6
T3B	610	7220	4640	54500	25.0	395	28.6
T4A	660	8380	4930	52300	34.0	378	63.1
T4B	680	7320	4930	53050	35.0	389	72.0
T5A	480	7280	4550	53930	32.5	381	88.8
T5B	550	7260	4680	53850	30.0	353	97.9
T6A	690	8080	5070	55900	37.5	394	50.0
T6B	700	8510	5020	53750	41.0	430	51.1
T7A	570	7440	4590	54150	42.5	359	103.2
T7B	720	7320	4600	53850	42.5	359	62.5
T8A	750	8900	5170	54200	40.0	305	51.1
T8B	720	8910	5070	54000	34.0	259	34.9
T9A	710	8750	4990	62500	45.0	330	26.7
T9B	700	8410	5160	64200	50.0	368	68.8
2A	663	6756	4685	66300	36.0	399	161.7
2B	622	7782	5028	66300	36.0	401	50.7
2C	657	7829	5043	66300	37.0	412	64.8
4A	707	6873	4726	66300	32.0	355	92.5
4B	648	6862	4722	66300	33.0	366	66.0
4C	637	6556	4615	66300	30.0	332	28.0
6A	654	6412	4193	66300	36.0	396	78.9
6B	666	7051	4786	66300	38.0	422	57.9
6C	592	7417	4909	66300	35.0	389	38.9
1	607	7181	4828	65220	41.0	455	135.0
2	643	7934	5077	65700	38.0	424	118.1
3	648	7840	5047	69720	37.0	412	84.6
4	628	7545	4951	66260	35.0	389	248.9
5	634	6956	4754	70200	35.5	394	67.7
6	713	8052	5115	66020	34.4	379	45.3
7	663	7486	4932	68030	35.0	389	73.9

* Measured

$$E_s = 29 \times 10^6 \text{ psi}$$

TABLE 3 RELATIONSHIPS OF CRACKING, SPLIT AND COMPRESSIVE STRENGTHS

Specimen Number	$\frac{f_{cr}}{f'_{sp}}$	$\frac{f_{cr}}{\sqrt{f'_c}}$	R
T1A	0.62	4.36	0.94
T1B	0.63	4.47	0.85
T2A	0.68	4.52	0.93
T2B	0.62	4.58	0.85
T3A	0.71	4.66	0.96
T3B	0.65	4.65	0.87
T4A	0.57	4.13	0.77
T4B	0.57	4.55	0.71
T5A	0.79	4.47	0.81
T5B	0.64	4.14	0.74
T6A	0.57	4.38	0.73
T6B	0.61	4.66	0.67
T7A	0.63	4.16	0.67
T7B	0.50	4.20	0.62
T8A	0.41	3.23	0.62
T8B	0.36	2.74	0.58
T9A	0.46	3.53	0.59
T9B	0.53	4.01	0.56
2A	0.60	4.85	0.47
2B	0.64	4.55	0.47
2C	0.63	4.66	0.47
4A	0.50	4.28	0.94
4B	0.56	4.42	0.94
4C	0.52	4.10	0.94
6A	0.61	4.95	1.42
6B	0.63	5.03	1.42
6C	0.66	4.52	1.42
1	0.75	5.37	2.00
2	0.66	4.76	7.08
3	0.64	4.65	0.38
4	0.62	4.48	0.76
5	0.62	4.72	1.15
6	0.53	4.22	2.00
7	0.59	4.50	5.73
Mean	0.60	4.40	
Std. Dev.	0.087	0.4907	
C.O.V.	14.59%	11.16%	

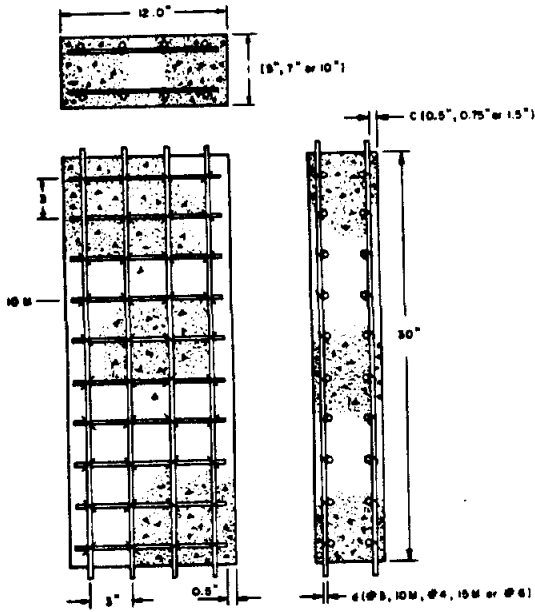


Figure 1 Reinforcement details of a typical specimen

Figure 2 Test set up and instrumentation

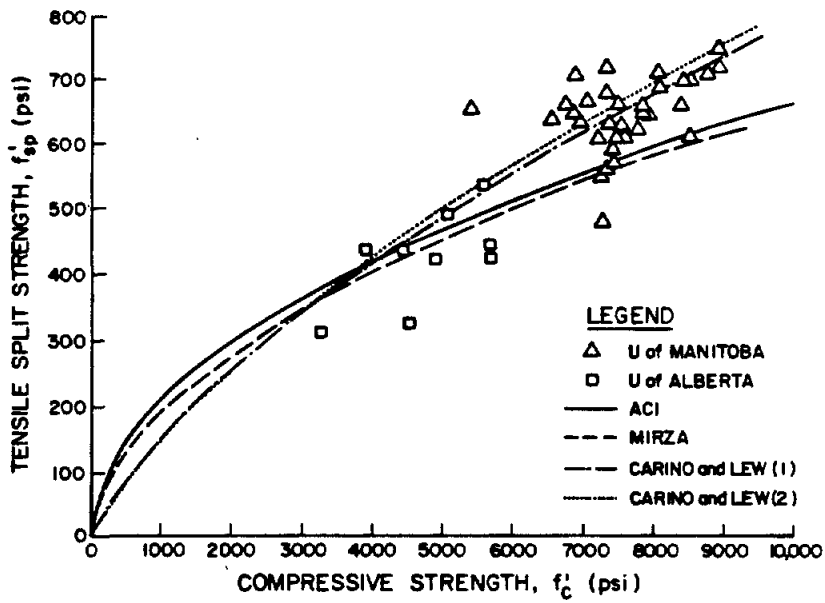
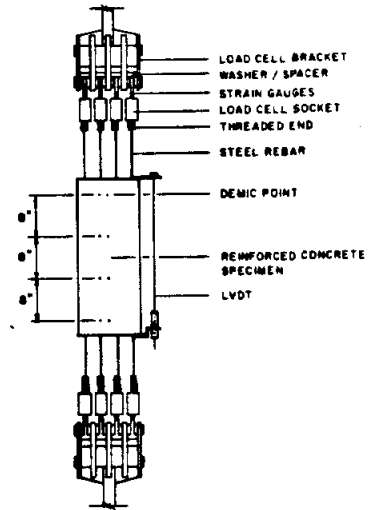


Figure 3 Tensile split versus compressive strengths

Figure 4 Load-gross strain relationship for typical specimen No. 2

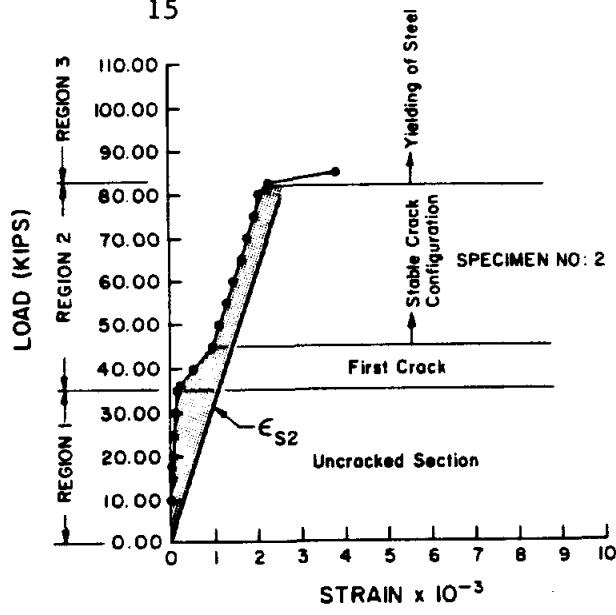


Figure 5 Relationship of cracking strength and tensile split strength

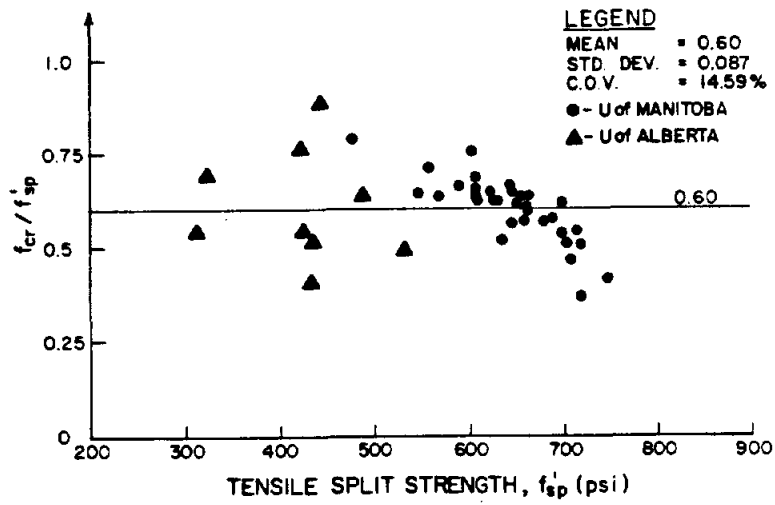
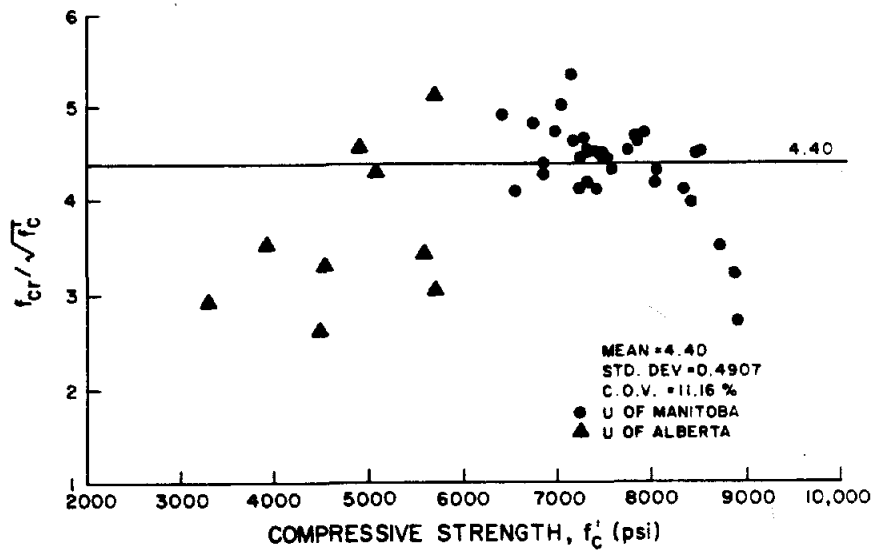


Figure 6 Relationship of cracking strength and $\sqrt{f'_c}$



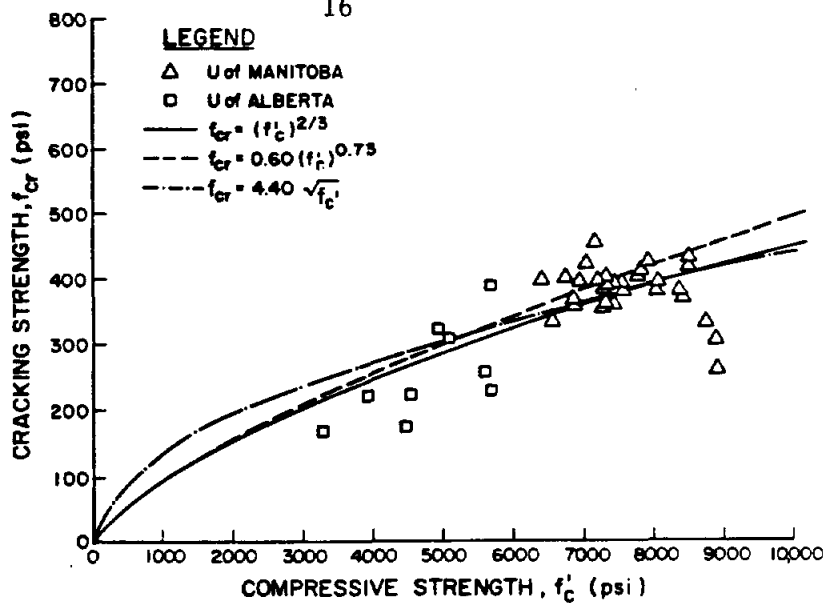


Figure 7 Cracking strength and compressive strength

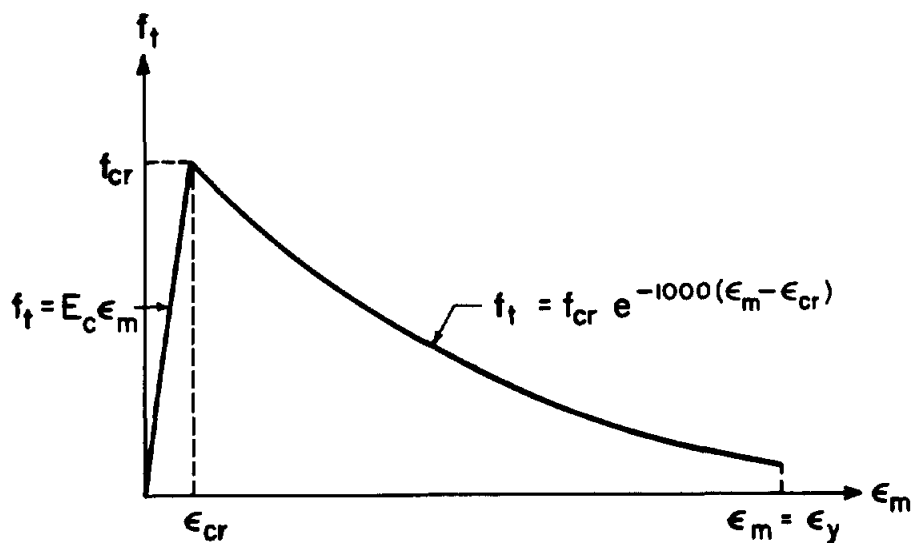


Figure 8 Proposed effective tensile stress-strain curve for concrete

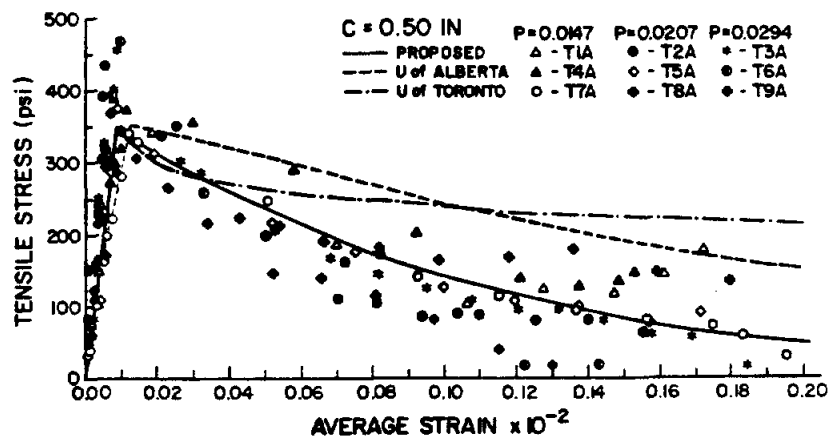


Figure 9(a) Comparison between measured and predicted concrete stress-strain curves for Specimens T1A-T9A

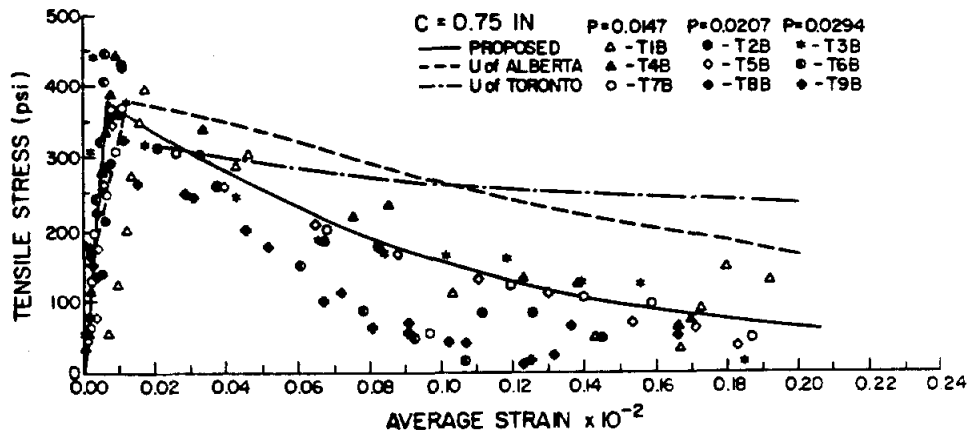


Figure 9(b) Comparison between measured and predicted concrete stress-strain curves for Specimens T1B-T9B

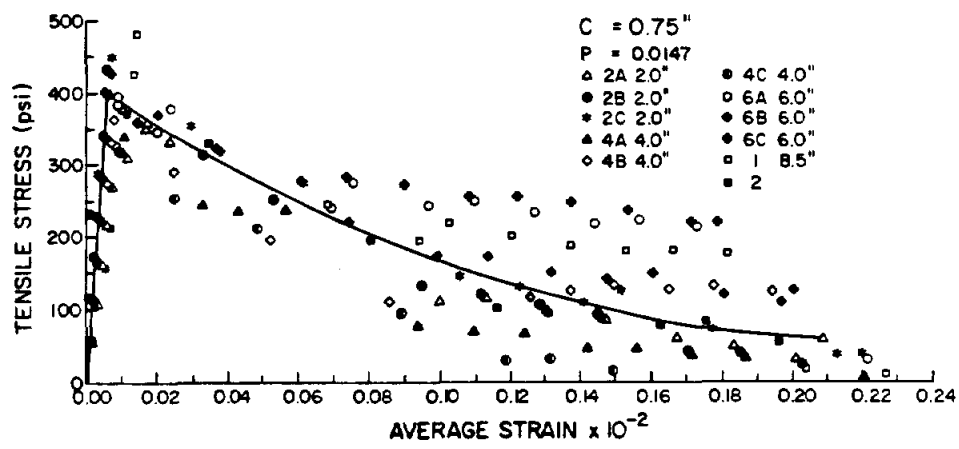


Figure 10(a) Effects of transverse reinforcement spacing on stress-strain curves for specimens with concrete cover of 0.75"

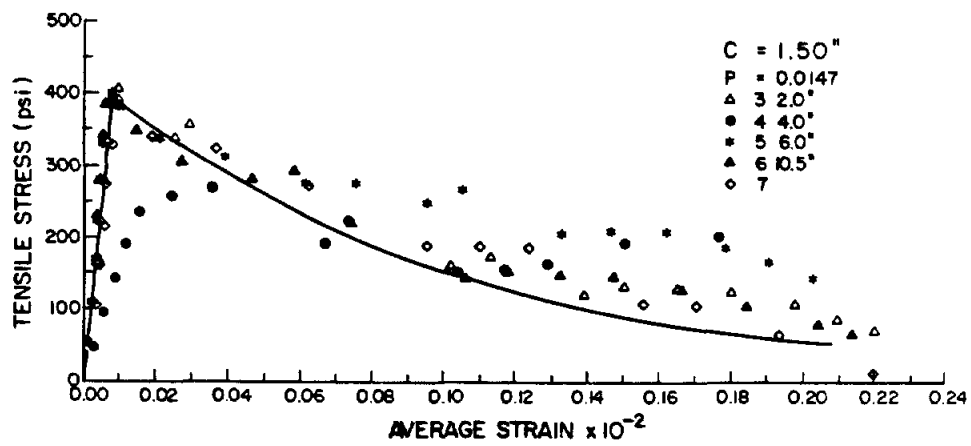
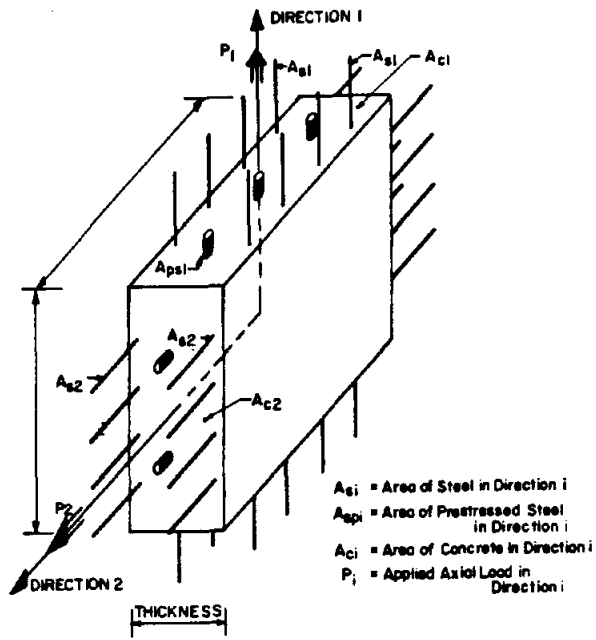
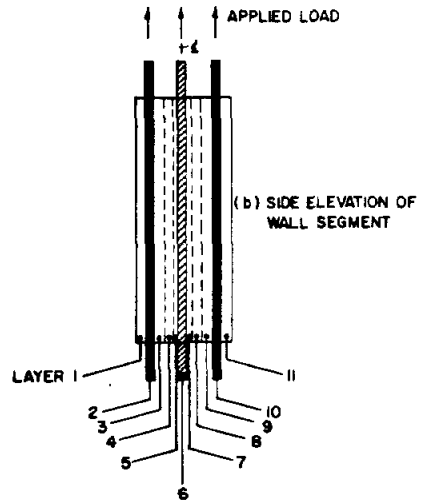


Figure 10(b) Effects of transverse reinforcement spacing on stress-strain curves for specimens with concrete cover of 1.50"



(a) SEGMENT REFERENCE DIRECTIONS



LAYERS	MATERIAL
1, 3, 4, 5, 7, 8, 9, 11	CONCRETE (A_{c1})
2, 10	REINFORCING STEEL (A_{s1})
6	PRE-STRESSING STEEL (A_{ps1})

(c) DETAILS OF LAYERS

Figure 11 Segment layering

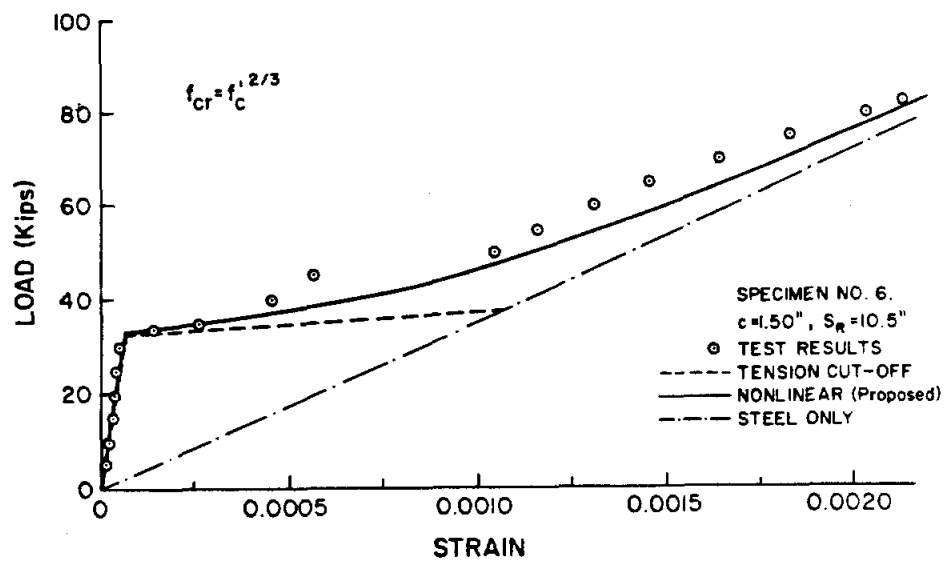


Figure 12 Load strain curve for specimen 6

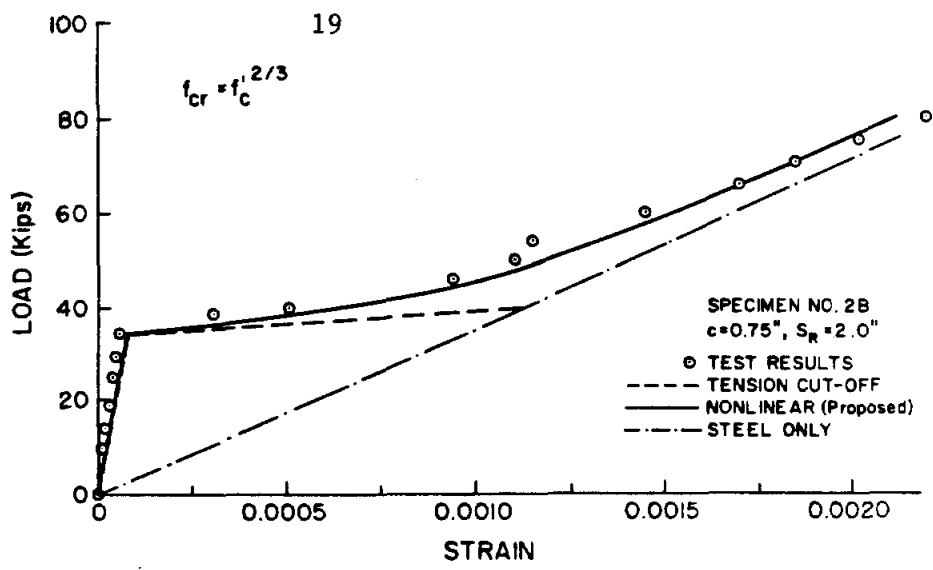


Figure 13 Load strain curve for specimen 2B

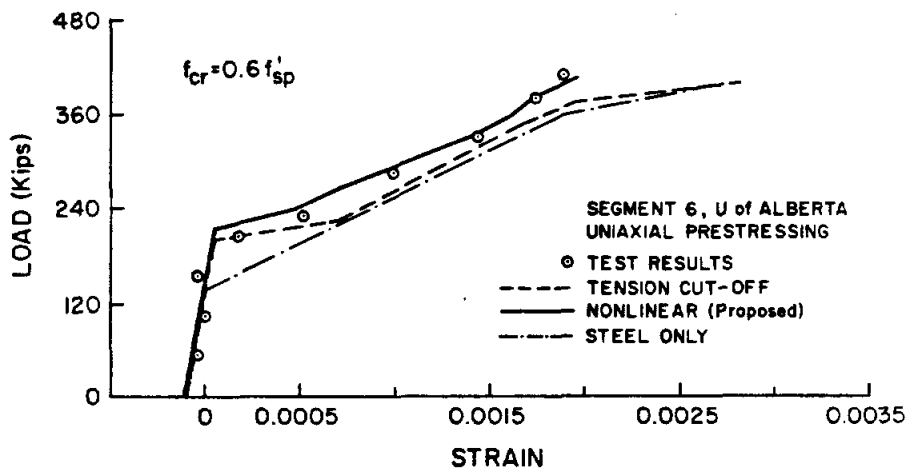


Figure 14 Load strain curve for segment 6

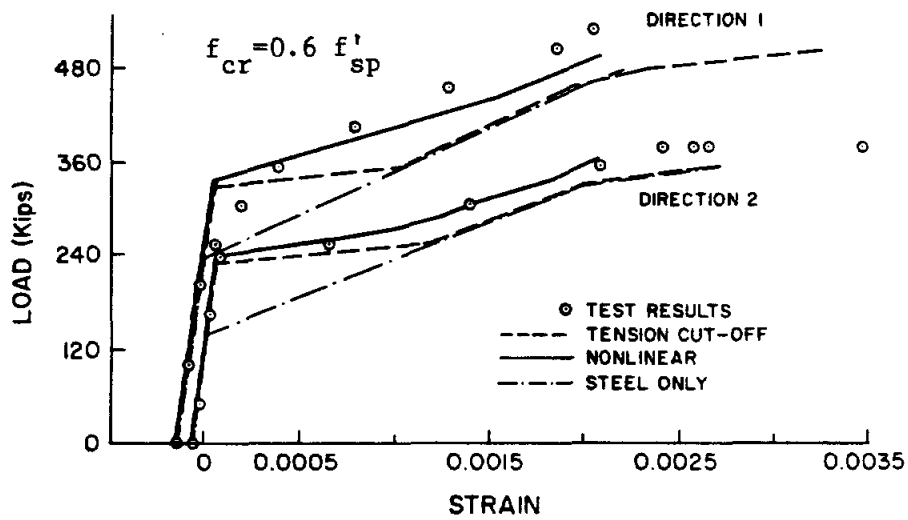


Figure 15 Load strain curve for segment 1